Science of the Total Environment 443 (2013) 896–903

Contents lists available at SciVerse ScienceDirect

Science of the Total Environment

journal homepage: www.elsevier.com/locate/scitotenv

Phototransformation rate constants of PAHs associated with soot particles

Daekyun Kim [a,*], Thomas M. Young [a,b], Cort Anastasio [a,c]

[a] Agricultural and Environmental Chemistry Graduate Group, University of California, One Shields Avenue, Davis, CA 95616, USA
[b] Department of Civil and Environmental Engineering, University of California, One Shields Avenue, Davis, CA 95616, USA
[c] Department of Land, Air, and Water Resources, University of California, One Shields Avenue, Davis, CA 95616, USA

HIGHLIGHTS

- PAHs on soot were evaluated by a model of coupled photolysis and diffusion.
- Photodegradation rate at the surface, diffusion coefficient, and light penetration path were determined.
- Low MW PAHs were influenced by fast photodegradation and fast diffusion.
- High MW PAHs were controlled either by slow photodegradation and slow diffusion or by diffusion alone.
- Fitted parameters were useful for describing empirical results of photodegradation of PAHs on soot.

ARTICLE INFO

Article history:
Received 10 July 2012
Received in revised form 13 November 2012
Accepted 13 November 2012
Available online 17 December 2012

Keywords:
PAHs
Soot
Diffusion
Photodegradation
Kinetics
Characteristic time

ABSTRACT

Photodegradation is a key process governing the residence time and fate of polycyclic aromatic hydrocarbons (PAHs) in particles, both in the atmosphere and after deposition. We have measured photodegradation rate constants of PAHs in bulk deposits of soot particles illuminated with simulated sunlight. The photodegradation rate constants at the surface (k_p^0), the effective diffusion coefficients (D_{eff}), and the light penetration depths ($z_{0.5}$) for PAHs on soot layers of variable thickness were determined by fitting experimental data with a model of coupled photolysis and diffusion. The overall disappearance rates of irradiated low molecular weight PAHs (with 2–3 rings) on soot particles were influenced by fast photodegradation and fast diffusion kinetics, while those of high molecular weight PAHs (with 4 or more rings) were apparently controlled by either the combination of slow photodegradation and slow diffusion kinetics or by very slow diffusion kinetics alone. The value of $z_{0.5}$ is more sensitive to the soot layer thickness than the k_p^0 value. As the thickness of the soot layer increases, the $z_{0.5}$ values increase, but the k_p^0 values are almost constant. The effective diffusion coefficients calculated from dark experiments are generally higher than those from the model fitting method for illumination experiments. Due to the correlation between k_p^0 and $z_{0.5}$ in thinner layers, D_{eff} should be estimated by an independent method for better accuracy. Despite some limitations of the model used in this study, the fitted parameters were useful for describing empirical results of photodegradation of soot-associated PAHs.

1. Introduction

Polycyclic aromatic hydrocarbons (PAHs) are ubiquitous hydrophobic organic pollutants generated mainly by anthropogenic combustion, although certain natural events such as forest fires are sometimes also important (Nikolaou et al., 1984). PAHs emitted to the atmosphere are likely in the gas phase initially, but nearly all subsequently condense on aerosol and terrestrial surfaces at ambient temperatures (Gustafson and Dickhut, 1997). In addition to PAHs, soot particles are also produced during combustion, from volatile species formed within flames that subsequently produce carbon-rich material through a complex mass growth process (Schmidt and Noack, 2000). Pyrogenic PAHs are suggested to be partially occluded in the soot matrix during the incomplete combustion process, to be trapped in micropores, or to have extremely high affinities for the aromatic flat surfaces of soot (Readman et al., 1984; Eganhouse, 1997).

Photodegradation is an important process for determining the residence time and fate of PAHs sorbed on various substrates, including soot and other atmospheric particles (Douben, 2003; Kamens et al., 1998). Numerous studies show that both direct and indirect phototransformation reactions of PAHs may proceed at different rates on particles compared to homogeneous or heterogeneous aqueous systems (Behymer and Hites, 1988; Pennise and Kamens, 1996; Miller and Olejnik, 2001; Matuzawa et al., 2001; Kahan and Donaldson, 2007; Jacobs et al., 2008). Although photodegradation

* Corresponding author at: Department of Environmental Engineering and Earth Sciences, Clemson University, 342 Computer Court, Anderson, SC 29625, USA. Tel.: +1 864 6561005; fax: +1 864 6560672.
E-mail address: daekyuk@clemson.edu (D. Kim).

0048-9697/$ – see front matter © 2012 Elsevier B.V. All rights reserved.
http://dx.doi.org/10.1016/j.scitotenv.2012.11.055

on soot particles is likely a large sink for PAHs, it is difficult to measure this process experimentally because it depends on the thickness of the soot deposit and, in most cases, on transport kinetics, which need to be considered. Several studies have measured PAH photodegradation rates on a variety of particle types and other solid substrates (Behymer and Hites, 1985; Pennise and Kamens, 1996; Matuzawa et al., 2001; Wang et al., 2005; Niu et al., 2007). However, these past studies suffer from one or two general weaknesses: (1) PAHs were added to an existing particle, typically at high concentrations, which does not mimic ambient particles, and (2) the reactions were examined in bulk (i.e., not on suspended particles) and the data treatment did not account for light attenuation by the particles, which will reduce the apparent photodegradation rate. The limited penetration depth of light may cause the formation of a PAH concentration gradient within a few micrometers of the medium surface over the course of a photodegradation experiment. This gradient, which cannot be directly measured over such a small depth interval, will induce diffusive transport of the PAH toward the irradiated surface. More importantly, the gradient causes an underestimation of the true photodegradation rate. Therefore, only a model that includes photodegradation, light attenuation, and diffusion can correctly describe the observed disappearance of PAHs (or other compounds) where ever the layer thickness is large in comparison to the light penetration depth.

One past approach that has included these three parameters is that of Balmer et al. (2000), who examined the photochemistry of pesticides on soils. In their work they considered that the temporal change in total mass M_{tot} of an illuminated compound in some substrate (e.g., soil) would be

$$\frac{dM_{tot}}{dt} = A \cdot \rho_{bulk} \cdot \int_{z=0}^{z=z_{tot}} \left[D_{eff} \cdot \frac{\partial^2 C(z)}{\partial z^2} - k_p^0 \cdot e^{-z/(z_{0.5}/\ln 2)} C(z) dz \right] \quad (1)$$

where A is the area of the layer, ρ_{bulk} is the bulk density of the substrate, D_{eff} is the effective diffusion coefficient of the compound, $C(z)$ is the concentration of the compound (mass of compound per mass substrate) at depth z, k_p^0 is the photodegradation rate constant of the compound at the surface, $z_{0.5}$ is the depth into the substrate where the light is attenuated by half compared to at the surface, and z_{tot} is the total layer thickness.

In this work we apply the same approach, but for PAH photodegradation in bulk deposits of soot particles collected onto Teflon filters, using our recently published disappearance profiles of illuminated PAHs on soot (Kim et al., 2009). Applying Eq. (1) to our PAH photodegradation experiments we are able to distinguish between the effects of diffusion and photodegradation to quantify the PAH photodegradation rate constants at the surface of soot (k_p^0), the effective diffusion coefficient of PAHs in our soot matrix (D_{eff}), and the light penetration depth ($z_{0.5}$) for different soot loadings.

2. Experiment methodology

2.1. Chemicals, photoreaction of soot samples, and PAH analysis

Soot particles were obtained from a rich premixed ethylene flame stabilized on a standard laboratory circular flat burner (McKenna Products, Inc., Pittsburg, CA). A mixture of ethylene and filtered air with an equivalence ratio of 1.73 (C/O = 0.58) was delivered to the burner at a total flow rate of 9.7 L min^{-1} (Kim et al., 2009). The particles were rich in organic carbon (approximately 60% of the total C was organic, while 40% was elemental) and contained a total PAH concentration of approximately 51 μg mg^{-1} for the 16 species that we analyzed. Soot particles were collected onto PTFE Teflon filters, with different particle masses (i.e., different layer thicknesses) for different samples. The disappearance rates of 16 PAHs sorbed on this soot were monitored using a Hewlett-Packard 6890 gas chromatograph and a Hewlett-Packard 5973 mass selective detector. The flat and relatively thin layers of soot particles on filters were illuminated from the top with output from a high pressure 1000-W xenon arc lamp after it was passed through a dichroic cold mirror in the lamp housing (to only transmit wavelengths between 300 and 500 nm). Photon flux values in each experiment were monitored by measuring the rate constant for loss of aqueous 2-nitrobenzaldehyde (2NB) as a chemical actinometer. The average first order rate constant for 2NB loss in the solar simulator (0.016 s^{-1}) is approximately 20% higher than the measured value in Davis, California, USA, at solar noon on the summer solstice (0.013 s^{-1}; Anastasio and McGregor, 2001). The methods for the generation and illumination of the soot samples, and for the extraction and analysis of PAHs, have been described in detail elsewhere (Kim et al., 2009). The PAHs studied were: naphthalene (Naph), acenaphthylene (Acy), acenaphthene (Ace), fluorene (Flu), phenanthrene (Phe), anthracene (Ant), fluoranthene (Flt), pyrene (Pyr), benzo[*a*]anthracene (BaA), chrysene (Chry), benzo[*b*]fluoranthene (BbF), benzo[*k*]fluoranthene (BkF), benzo[*a*]pyrene (BaP), indeno[*1,2,3-cd*]pyrene (InP), dibenz[*a,h*]anthracene (DaA), and benzo[*g,h,i*]perylene (BgP). In the end, Naph was not included in the calculation of photodegradation rates and diffusion coefficients because its apparent degradation rates were inconsistent with soot thicknesses, probably because of its high volatility compared to the other PAHs. In addition, DaA was not included because its concentrations were below our method detection limit.

Prior research has shown that Acy, Ace, and Flu showed an obvious two-phase disappearance in all experiments while Phe and Ant exhibited this behavior for all but the highest soot loading experiments (Kim et al., 2009). The first phase loss was 5–40 times faster than the second phase and occurred within 3 h for Acy, Ace, and Flu, and within 10 h for Phe and Ant. Two-phase disappearance kinetics were not observed for any of the higher molecular weight PAHs (i.e., with 4–6 rings). We interpret this behavior to mean that: (1) for the higher molecular weight PAHs, the rate constant for photodegradation is slower than diffusion (i.e., mass transport of PAHs from deeper particle layers keeps pace with photolytic loss at the surface), while (2) for the lower molecular weight PAHs, the rate constant for photodegradation is faster than diffusion, leading to a rapid depletion in the first phase and slower, diffusion-controlled, loss in the second phase.

To apply Eq. (1), the soot layer thickness z_{tot}, the bulk soot density ρ_{bulk}, and the surface area A must be known. The thickness of the soot layer was calculated using the measured soot mass on each filter divided by the measured surface area of the sampled area (774 mm^2) and a literature value for the bulk density of soot (0.6 g/cm^3) (Rockne et al., 2000). The intrinsic photodegradation rate constant k_p^0 and the light penetration depth $z_{0.5}$ were then fitted for the three soot loading levels for which experimental data were available (Table 1).

2.2. Mathematical model solution

Eq. (1) was solved using an explicit forward-marching finite-difference solution implemented in Fortran 77 (Farlow, 1993). Boundary conditions for the equation were $C(0) = 0$ for $t > 0$ (i.e., the soot surface is in equilibrium with PAH-free room air) and $\partial C(z)/\partial z = 0$ at the filter-soot interface (i.e., the filter is an impenetrable boundary). As an initial condition we assumed a uniform distribution of each PAH in each soot sample. The Fortran program was typically run using 345,600 time steps and 200 spatial steps. This ensured that the stability criterion for the numerical solution (i.e., $D_{eff}\,\Delta t/\Delta z^2 < 0.5$) was always satisfied.

The accuracy of the numerical model was assessed by comparing it to an infinite series analytical solution for diffusion in a plane sheet for the case of a constant surface concentration and no reaction ($k_p^0 = 0$) (Crank, 1975). The numerical model and the truncated form of the infinite series analytical solution differed by less than

Table 1
The actual photodegradation rate constant, k_p^0, the effective diffusion constant, D_{eff}, and the light penetration depth, $z_{0.5}$, of PAHs obtained by fitting curves with experimental data at different soot loadings.

	2.1 mg soot (z_{tot} = 4.5 μm)				4.9 mg soot (z_{tot} = 11 μm)				12.7 mg soot (z_{tot} = 27 μm)			
	k_p^0 (h^{-1})	D_{eff} (cm^2/s)	$z_{0.5}$ (μm)	Cal'd error[c]	k_p^0 (h^{-1})	D_{eff} (cm^2/s)	$z_{0.5}$ (μm)	Cal'd error[c]	k_p^0 (h^{-1})	D_{eff} (cm^2/s)	$z_{0.5}$ (μm)	Cal'd error[c]
Acy	6.2 (0.37*/0.026**)[a]	2.1E−13 1.1E−12[b]	0.5	0.04	6.2 (0.80*/0.030**)[a]	4.1E−13	1.5	0.07	6.3 (0.47*/0.022**)[a]	4.2E−13 6.0E−11[b]	3.4	0.07
Ace	6.4 (0.37*/0.024**)[a]	2.1E−13 1.4E−12[b]	0.5	0.04	6.3 (0.44*/0.033**)[a]	4.0E−13	1.2	0.07	6.4 (0.54*/0.014**)[a]	4.3E−13 5.7E−11[b]	3.6	0.07
Flu	3.6 (0.33*/0.025**)[a]	2.0E−13 6.6E−13[b]	0.6	0.04	3.6 (0.54*/0.028**)[a]	1.2E−12	1.5	0.10	3.6 (0.18*/0.033**)[a]	4.0E−12 2.2E−11[b]	2.8	0.03
Phe	2.5 (0.19*/0.021**)[a]	8.0E−13 4.2E−13[b]	0.6	0.02	2.5 (0.19*/0.043**)[a]	1.3E−12	1.5	0.01	2.5 (0.043)[a]	2.0E−12 7.8E−12[b]	2.5	0.07
Ant	2.7 (0.18*/0.017**)[a]	2.5E−13 1.3E−13[b]	0.6	0.02	2.7 (0.16*/0.035**)[a]	1.1E−12	1.4	0.01	2.7 (0.051)[a]	2.0E−12 7.1E−12[b]	2.8	0.14
Flt	0.025 (0.043)[a]	8.0E−13 2.9E−14[b]	1.4	0.03	0.029 (0.025)[a]	9.5E−13	2.4	0.02	0.029 (0.006)[a]	9.0E−13 1.0E−12[b]	2.4	0.01
Pyr	0.022 (0.045)[a]	7.0E−13 2.9E−14[b]	1.4	0.02	0.022 (0.027)[a]	1.4E−12	3.2	0.01	0.022 (0.008)[a]	1.6E−12 1.0E−12[b]	3.6	0.02
BaA	1.4E−3 (0.012)[a]	1.0E−13	0.2	0.01	1.4E−3 (0.016)[a]	1.4E−12	6.0	0.03	1.4E−3 (0.006)[a]	2.0E−12 4.9E−12[b]	7.0	0.02
Chry	2.2E−4 (0.005)[a]	7.0E−14	0.1	0.05	2.2E−4 (0.007)[a]	1.8E−13	0.8	0.01	2.2E−4 (≪0.001)[a]	2.0E−13 5.7E−11[b]	1.0	0.04
BbF	3.2E−4 (0.008)[a]	2.0E−13	0.3	0.05	3.2E−4 (0.006)[a]	1.7E−13	0.6	0.04	3.2E−4 (≪0.001)[a]	3.0E−12 2.2E−11[b]	1.4	0.02
BkF	2.9E−4 (0.013)[a]	2.0E−13	0.3	0.01	2.9E−4 (0.008)[a]	3.0E−13	0.6	0.06	2.9E−4 (0.001)[a]	1.5E−12 7.8E−12[b]	3.5	0.03
BaP	2.9E−4 (0.016)[a]	2.0E−13	0.4	<0.01	2.9E−4 (0.012)[a]	1.2E−12	2.5	0.01	2.9E−4 (0.003)[a]	1.8E−12 7.1E−12[b]	6.0	0.01
InP	1.1E−4 (0.003)[a]	2.0E−14	<0.1	0.01	1.1E−4 (0.001)[a]	7.5E−13	0.6	0.02	1.1E−4 (≪0.001)[a]	1.0E−12 1.0E−12[b]	1.0	0.02
BgP	9.0E−6 (0.045)[a]	2.0E−14	<0.1	0.01	9.0E−6 (0.007)[a]	1.1E−12	1.3	0.04	9.0E−6 (0.002)[a]	8.0E−13 1.0E−12[b]	4.4	0.02

[a] Empirical disappearance rate constant calculated from the observed bulk kinetics: *for the first phase loss, **for the second phase loss (Kim et al., 2009).
[b] Effective diffusion coefficients calculated from dark control experiments (not available for some PAHs in the 2.1 mg soot sample or for any PAH in the 4.9 mg soot sample).
[c] Σ (observed value of relative mass-fitted value of relative mass)^2.

0.8% for the entire range of diffusion coefficients observed in this study.

2.3. Parameter estimation

Optimal values of D_{eff}, k_p^0, and $z_{0.5}$ for the PAHs sorbed on soot layers of different thicknesses were determined using Eq. (1) under illumination conditions by minimizing the squared deviations between the model and empirical degradation data. For the purpose of comparison, D_{eff} values were also obtained by fitting dark control experiments using the analytical solution of the diffusion equation (i.e., Eq. (1) with $k_p^0 = 0$).

2.4. Characteristic times

In order to quantitatively compare the relative importance of photodegradation and diffusion, the characteristic times for photodegradation and diffusion of PAHs on soot with various

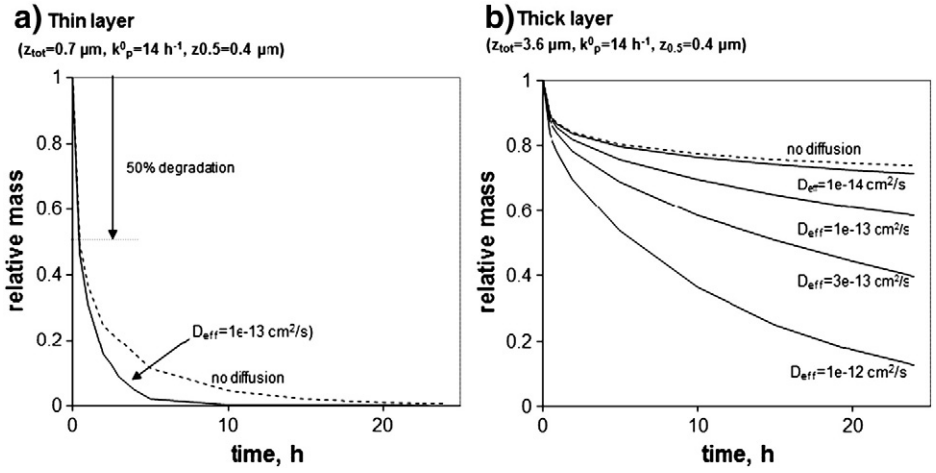

Fig. 1. Hypothetical examples of photodegradation of PAHs in a thin soot layer (a) and a thick layer (b). Solid lines show the cases where both photodegradation and diffusion are occurring, while dashed lines (no diffusion) show PAH loss for the case with direct photodegradation only.

Table 2
Characteristic times for diffusion (t_{Diff}) and photodegradation ($t_{h\nu}$) of PAHs in illuminated soot layers of various thicknesses.

	2.1 mg soot (z_{tot} = 4.5 μm)			4.9 mg soot (z_{tot} = 11 μm)			12.7 mg soot (z_{tot} = 27 μm)		
	t_{Diff}, s	$t_{h\nu}$, s	$t_{Diff}/t_{h\nu}$[a]	t_{Diff}, s	$t_{h\nu}$, s	$t_{Diff}/t_{h\nu}$[a]	t_{Diff}, s	$t_{h\nu}$, s	$t_{Diff}/t_{h\nu}$[a]
Acy	4.8E+05	3.6E+03	*1.3E+02*	1.5E+06	2.9E+03	*5.1E+02*	8.7E+06	3.1E+03	*2.8E+03*
Ace	4.8E+05	3.5E+03	*1.4E+02*	1.5E+06	3.6E+03	*4.2E+02*	8.5E+06	2.9E+03	*2.9E+03*
Flu	5.1E+05	5.2E+03	*9.8E+01*	5.0E+05	5.1E+03	*1.0E+02*	9.1E+05	6.7E+03	*1.4E+02*
Phe	1.3E+05	7.4E+03	*1.7E+01*	4.7E+05	7.3E+03	*6.4E+01*	1.8E+06	1.1E+04	*1.7E+02*
Ant	4.1E+05	6.9E+03	*5.9E+01*	5.5E+05	4.1E+03	*1.4E+02*	1.8E+06	8.9E+03	*2.0E+02*
Flt	1.3E+05	2.9E+05	4.4E−01	6.4E+05	6.7E+05	9.5E−01	4.1E+06	9.7E+05	4.2E+00
Pyr	1.5E+05	3.3E+05	4.5E−01	4.3E+05	3.5E+05	1.2E+00	2.3E+06	8.5E+05	2.7E+00
BaA	1.0E+05	3.9E+07	2.6E−03	4.3E+05	2.3E+06	1.9E−01	1.8E+06	6.2E+06	2.9E−01
Chry	1.5E+06	6.5E+08	2.2E−03	3.4E+06	1.6E+08	2.1E−02	1.8E+07	3.1E+08	5.8E−02
BbF	5.1E+05	1.2E+08	4.4E−03	3.6E+06	1.4E+08	2.5E−02	1.2E+06	1.5E+08	8.2E−03
BkF	5.1E+05	1.3E+08	3.9E−03	2.0E+06	1.6E+08	1.3E−02	2.4E+06	6.7E+07	3.7E−02
BaP	5.1E+05	9.7E+07	5.2E−03	5.0E+05	3.6E+07	1.4E−02	2.0E+06	3.7E+07	5.4E−02
InP	5.1E+06	5.2E+09	9.7E−04	8.1E+05	4.2E+08	1.9E−03	3.7E+06	6.2E+08	5.8E−03
BgP	5.1E+06	3.1E+10	1.6E−04	5.5E+05	2.3E+09	2.4E−04	4.6E+06	1.7E+09	2.7E−03

[a] The ratio $t_{Diff}/t_{h\nu}$ indicates whether diffusion might limit photodegradation, with values ≫ 1 (in italics) indicating significant limitation, and values ≪ 1 indicating no limitation.

thicknesses were calculated. The diffusion characteristic time (t_{Diff}) and photodegradation characteristic time ($t_{h\nu}$) were obtained using:

$$t_{Diff} = z_{tot}^2 / 2D_{eff} \quad (2)$$

$$t_{h\nu} = \left(1 / \int_{z=0}^{z=z_{tot}} k_p dz \times z_{tot}\right). \quad (3)$$

3. Results and discussion

3.1. Coupled photolysis and diffusion

As described in the previous section, the overall rate of disappearance of PAHs in an irradiated porous layer not only depends on the phototransformation rate constant (which governs photochemical

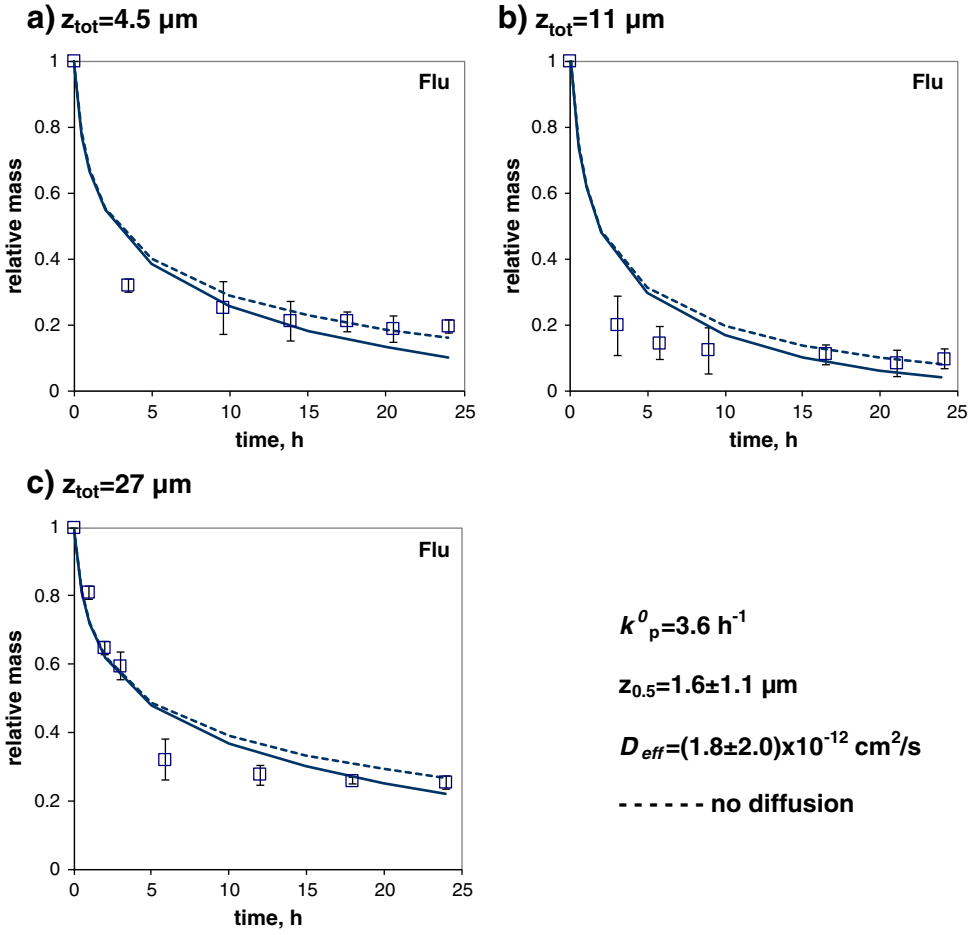

Fig. 2. Fitting of coupled photodegradation and diffusion for Flu on soot layers of various thicknesses. The solid lines correspond to the fitted model, while the dashed lines represent a separate model fit of the same values for k_p^0, and $z_{0.5}$ but with D_{eff} set to zero. Errors are one standard deviation.

loss in the illuminated, upper portion of the sample) but also on the diffusion rate (which governs mass transport from deeper layers to upper, illuminated layers). Therefore, in general, the disappearance rate constant observed in an experiment will be lower than the actual photodegradation rate constant because of light attenuation by particles unless the layer thickness approaches zero and/or the rate of diffusion substantially exceeds the rate of phototransformation. Some hypothetical examples of bulk PAH loss (expressed as relative mass, i.e., $M_t/M_{t=0}$) calculated with Eq. (1) are shown in Fig. 1; these illustrate the influence of diffusion and photodegradation with a thin and a thick layer on the observed disappearance rates of PAHs. The upper dashed lines represent a case with no diffusion (i.e., $D_{eff}=0$) and the solid lines show cases for different rates of diffusion.

Fig. 1a shows that for a PAH in a relatively thin layer (e.g., $z_{tot}=0.7$ μm) of soot, where there is less attenuation of light over the depth of the soot deposit, the bulk rate of decay is relatively fast and diffusion plays only a small role. Therefore, for thinner layers the actual photodegradation curve can be approximated by assuming rapid diffusion, especially at shorter illumination times. In a thicker layer of soot, however, the apparent photodegradation rates of PAHs can be strongly influenced by diffusion. As shown in Fig. 1b, photodegradation depletes PAHs in the near-surface layers of soot, but PAHs in deeper layers — where there is much less light — are protected from photodegradation until they diffuse into the near-surface layers. In this case the observed, bulk photodegradation rate is very dependent upon the diffusion coefficient of the PAH. Hence, measured bulk disappearance curves cannot be used to determine the intrinsic photolytic behaviors of PAHs without considering diffusion.

3.2. Evaluation of fitting parameters

Fitting Eq. (1) to our experimental data for each PAH for each of the three different soot loadings gives three best-fit parameters: the intrinsic photodegradation rate constant (i.e., the rate constant at the surface of the soot, k_p^0), the effective diffusion coefficient (D_{eff}), and the depth in the soot layer at which the photon flux is half of the surface value ($z_{0.5}$). These results are compiled in Table 1. Calculated errors were given by the sum of the squared differences between observed and fitted values of relative mass for each PAH.

The best-fit k_p^0 values for a given PAH are essentially constant — as they should be — across the three soot thicknesses, but the ranges for D_{eff} and $z_{0.5}$ (which we would also expect to be independent of layer thickness) are somewhat wider. As shown in Fig. 1, Eq. (1) is almost insensitive to the effective diffusion constant D_{eff} in thinner soot layers, which suggests that values derived from thicker layers are more accurate. However, the generally observed increase in D_{eff} with increasing soot thickness might be due to variations in tortuosity and solute adsorption in soot layers of various thicknesses.

In addition, past work has shown that k_p^0 and $z_{0.5}$ are strongly correlated and cannot be accurately determined separately (Balmer et al., 2000). Therefore, $z_{0.5}$ values determined for the thickest soot sample (27 μm) are likely more reliable than those determined for thinner layers. D_{eff} values for PAHs in the 2.1 mg and 4.9 mg soot samples calculated from dark control experiments are also listed in Table 1. The D_{eff} results from our independent method (dark controls) are generally greater than the fitted values from the photodegradation experiments with exceptions for Phe, Ant, Flt, and Pyr for 2.1 mg soot and only Pyr

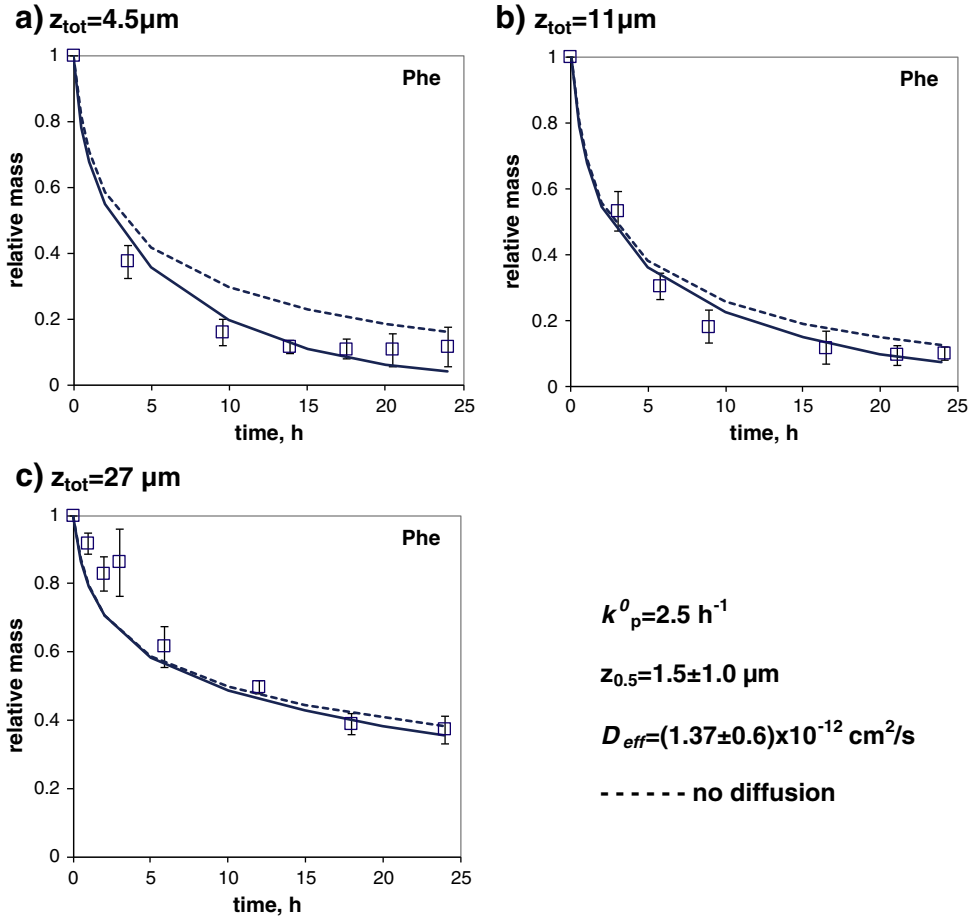

Fig. 3. Fitting of coupled photodegradation and diffusion for Phe on soot layers of various thicknesses. The solid lines correspond to the fitted model, while the dashed lines represent a separate model fit of the same values for k_p^0, and $z_{0.5}$ but with D_{eff} set to zero. Errors are one standard deviation.

for 12.7 mg soot. As layer thickness increases, the fitted D_{eff} values showed more consistency than those from dark experiments.

As shown in Table 1, k_p^0 values are generally inversely correlated with the molecular weight of the PAHs: Acy and Ace, the lightest PAHs, showed the highest k_p^0 values (6.2–6.4 h^{-1}) while BgP, one of the heaviest PAHs we studied, has the lowest rate constant (9×10^{-6} h^{-1}). Comparing our calculated k_p^0 values for PAHs on soot (Table 1) with reported photodegradation rate constants for PAHs in aqueous solution shows different levels of agreement. For example, our k_p^0 values for Ace, Phe, and Ant (6.4, 2.5, and 2.7 h^{-1}, respectively) are 4–28 times higher than the rate constants measured in water (0.23, 0.11, and 0.66 h^{-1}, respectively) where a 100-W high pressure mercury lamp was used (Fukuda et al., 1988). In contrast, our k_p^0 values for Phe, Ant, Pyr, Chry, BaA, and BgP are much lower than photodegradation rate constants in methanol/water (50/50) where a 500-W medium pressure mercury lamp was used (Chen et al., 1996). Of course these photodegradation rate constants depend on the photon flux in each experimental system (which was not reported for the aqueous studies) as well as the wavelengths of irradiation (which differ between our study and the aqueous studies). Ram and Anastasio (2009) examined PAH loss on ice samples in the same illumination system that we used and found that quantum yields for PAH loss were similar to those in solution. Comparing their direct photodegradation rate constants for Phe, Flt, and Pyr (0.14, 0.05, and 1.0 h^{-1}, respectively) with ours (2.5, 0.025, and 0.022 h^{-1}, respectively) shows good agreement for Flt (within a factor of 2), but poor agreement for Phe and Pyr. Another puzzling component of our photodegradation results is that we find that k_p^0 decreases as molecular weight increases, while past studies in water have found the opposite (Haque, 1980; Fukuda et al., 1988; Frechse, 1991; Chen et al., 1996; Ram and Anastasio, 2009). The photodegradation of PAHs is affected by the presence of organic compounds in the particles (McDow et al., 1994) and also likely depends on the manner in which the PAHs are incorporated into the soot matrix. Collectively, these factors may account for the differences between our values and aqueous-phase values since our particles are rich in organic carbon.

Past work on photodegradation on soils showed higher $z_{0.5}$ values for pesticides whose light absorption maxima (λ_{max}) are at longer wavelengths, likely because the soil more strongly attenuates light at shorter wavelengths (Balmer et al., 2000). We do not see this behavior in our PAH photodegradation on soot — e.g., $z_{0.5}$ values for all PAHs in the thickest layer are similar (1.0–7.0 μm; Table 1). This is probably because light absorption by soot has very little wavelength dependence throughout the UV and visible regions where PAHs absorb.

Table 2 shows the characteristic times for photodegradation and diffusion of PAHs in soot obtained using Eqs. (2) and (3). The ratios of the characteristic times ($t_{Diff}/t_{h\nu}$) help us to determine how much diffusion might limit photodegradation; significant diffusion limitation is expected for $t_{Diff}/t_{h\nu}$ greater than 1, while values of $t_{Diff}/t_{h\nu}$ less than 1 indicate no diffusion limitation to photodegradation. Generally, diffusion characteristic times are similar for all of the PAHs studied, while the photodegradation characteristic time increases extensively with molecular size of the PAH (Table 2). In all cases, the photodegradation characteristic times ($t_{h\nu}$) of low molecular weight PAHs (from Acy to approximately Pyr) are less than their diffusion characteristic times (t_{Diff}), indicating that diffusion is slow compared to photodegradation and therefore limits the overall degradation rate. For high molecular weight PAHs, however, diffusion characteristic

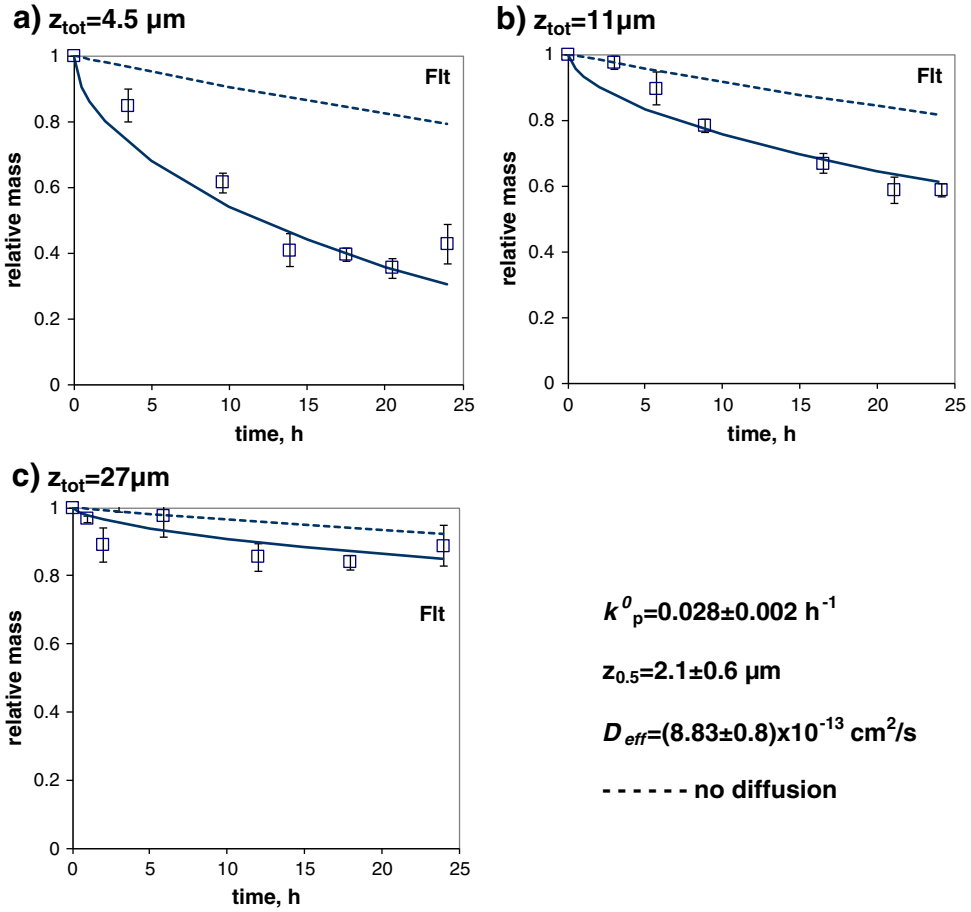

Fig. 4. Fitting of coupled photodegradation and diffusion for Flt on soot layers of various thicknesses. The solid lines correspond to the fitted model, while the dashed lines represent a separate model fit of the same values for k_p^0, and $z_{0.5}$ but with D_{eff} set to zero. Errors are one standard deviation.

times are much less than photodegradation characteristic times, suggesting that diffusion does not limit the overall disappearance rate.

3.3. Fitting of photodegradation data of selected PAHs

Here we focus on the kinetic results of Flu, Phe, and Flt, which epitomize the three different bulk photodegradation behaviors of PAHs that we have observed (Kim et al., 2009). Fig. 2 shows clearly the contributions of photodegradation and diffusion to the disappearance of Flu on soot. The solid lines represent the cases when both photodegradation and diffusion are considered and the dashed lines are calculated for the conditions of "no diffusion" (i.e., $D_{eff} = 0$). Throughout each soot deposit the solid and dashed lines are almost identical, indicating diffusion is slow compared to photodegradation. This is consistent with the characteristic time analysis: as shown in Table 2, the characteristic times for diffusion and photodegradation are $(5–9)\times10^5$ s and $(5–7)\times10^3$ s, respectively, indicating significant diffusion limitation (i.e., $t_{Diff}/t_{h\nu} \gg 1$). The intrinsic rate of Flu photodegradation determined in this study (3.6 h^{-1}; Table 1) is in the large range of values reported in the aqueous phase (1.5–21 h^{-1}) (Jacek and Dorota, 2001; Sabaté et al., 2001; Tham and Sakukawa, 2007).

The degradation data for Phe on irradiated soot layers of various thicknesses are shown in Fig. 3. The characteristic time analysis of the Phe data shows a similar picture to that of Flu: values of $t_{Diff}/t_{h\nu}$ for Phe for all three soot samples are greater than 1, indicating that diffusion limits photodegradation significantly (Table 2). As shown in Table 1, our previously measured first-phase photodegradation loss rate constants for both Flu and Phe are much lower than values of k_p^0 determined here from fitting the coupled photodegradation–diffusion model; this is because of a significant diffusion limitation to degradation. This same situation applies for most of the other small PAHs (Table 1) and again shows that diffusion must be considered to determine intrinsic photodegradation rate constants for PAHs in solid phases. Finally, our calculated intrinsic photodegradation rate constant for Phe on soot (2.5 h^{-1}) is near the middle of the very large range of values (0.11–21 h^{-1}) previously reported for Phe in aqueous solution (Fukuda et al., 1988; Sabaté et al., 2001).

The photodegradation of Flt (Fig. 4) is fairly different from those of Flu and Phe. In the case of Flt, the "no diffusion" curves are much higher than the coupled photodegradation–diffusion curves, indicating that the photodegradation of Flt in our experiments is less limited by diffusion, unlike the cases for Flu and Phe. This difference arises because photodegradation for Flt is much slower than for the other two PAHs (with a rate constant for Flt that is two orders of magnitude smaller), while the diffusion coefficients are similar for all three compounds (Table 1). The degradation of Flt on soot, therefore, is a combined process of relatively slow photodegradation with little mass transport limitation, consistent with the ratios of characteristic times, $t_{Diff}/t_{h\nu}$, which are all near 1 (Table 2).

4. Conclusions

Photolysis is an important elimination pathway for PAHs in particles in the environment, and the actual photolysis rate constants of PAHs associated with soot particles cannot be determined without understanding the contribution of diffusion kinetics within layers. For smaller PAHs (e.g., Flu and Phe), diffusion is slower than direct photolysis, while the photodegradation of Flt is less limited by diffusion. For all three of these compounds (as well as the other PAHs), the "apparent half-life" measured experimentally in soot will be longer than predicted from $\ln 2/k_p^0$ both because of diffusion limitations, but also because of attenuation of light in the soot layer. This work demonstrates the advantages and limitations of the selected experimental procedures and coupled photodegradation–diffusion model approach to assess photodegradation of PAHs on soot, which could be applied to many environmental compounds and substrates. In the specific case of PAHs, the lifetimes and fates of particulate PAHs will also be affected by other reactants and pathways, such as ozone, NO_x, and biota. Furthermore, soot particles deposited from the atmosphere can interact with soil and surface water, which will introduce a host of other reaction pathways.

Acknowledgments

We thank Ben Kumfer and Ian Kennedy for the soot samples. The project described was supported by grant number P42ES004699 from the National Institute of Environmental Health Sciences. The content is solely the responsibility of the authors and does not necessarily represent the official views of the National Institute of Environmental Health Sciences or the National Institutes of Health.

References

Anastasio C, McGregor KG. Chemistry of fog waters in California's Central Valley: 1. In situ photoformation of hydroxyl radical and singlet molecular oxygen. Atmos Environ 2001;35:1079–89.
Balmer ME, Goss KU, Schwarzenbach RP. Photolytic transformation of organic pollutants on soil surfaces—an experimental approach. Environ Sci Technol 2000;34:1240–5.
Behymer TD, Hites RA. Photolysis of polycyclic aromatic hydrocarbons adsorbed on simulated atmospheric particulates. Environ Sci Technol 1985;19:1004–6.
Behymer TD, Hites RA. Photolysis of polycyclic aromatic hydrocarbons on fly ash. Environ Sci Technol 1988;22:1311–9.
Chen JW, Kong LR, Zhu CM, Huang QG, Wang LS. Correlation between photolysis rate constants of polycyclic aromatic hydrocarbons and frontier molecular orbital energy. Chemosphere 1996;33:1143–50.
Crank J. The mathematics of diffusion. 2nd ed. Oxford: Clarendon Press; 1975.
Douben PET. PAHs: an ecotoxicological perspective. Chichester: John Wiley & Sons; 2003.
Eganhouse RP. Molecular markers in environmental geochemistry. Washington DC: American Chemical Society; 1997.
Farlow SJ. Partial differential equations for scientists and engineers. 2nd ed. New York: Dover publications; 1993.
Frechse H. Pesticide chemistry: advances in international research, development, and legislation. VCH: Weinheim; 1991.
Fukuda K, Inagaki Y, Maruyama T, Kojima HI, Yoshisa T. On the photolysis of alkylated naphthalenes in aquatic systems. Chemosphere 1988;17:651–9.
Gustafson KE, Dickhut RM. Particle/gas concentrations and distributions of PAHs in the atmosphere of Southern Chesapeake Bay. Environ Sci Technol 1997;31:140–7.
Haque R. Dynamics, exposure and hazard assessment of toxic chemicals. Ann Arbor: Ann Arbor Science Publishers Inc.; 1980.
Jacek SM, Dorota O. Photolysis of polycyclic aromatic hydrocarbons in water. Water Res 2001;35:233–43.
Jacobs LE, Weavers LK, Chin YP. Direct and indirect photolysis of polycyclic aromatic hydrocarbons in nitrate-rich surface waters. Environ Toxicol Chem 2008;27:1643–8.
Kahan TF, Donaldson DJ. Photolysis of polycyclic aromatic hydrocarbons on water and ice surfaces. J Phys Chem A 2007;111:1277–85.
Kamens RM, Guo Z, Fulcher JN, Bell DA. Influence of humidity, sunlight, and temperature on the daytime decay of polyaromatic hydrocarbons on atmospheric soot particles. Environ Sci Technol 1998;22:103–8.
Kim D, Kumfer BM, Anastasio C, Kennedy IM, Young TM. Environmental aging of polycyclic aromatic hydrocarbons on soot and its effect on source identification. Chemosphere 2009;76:1075–81.
Matuzawa S, Nasser-Ali L, Garrigues P. Photolytic behavior of polycyclic aromatic hydrocarbons in diesel particulate matter deposited on the ground. Environ Sci Technol 2001;35:3139–43.
McDow SR, Sun QR, Vartialnen M, Hong YS, Yao YL, Fister T, et al. Effect of composition and state of organic components on polycyclic aromatic hydrocarbon decay in atmospheric aerosols. Environ Sci Technol 1994;28:2147–53.
Miller JS, Olejnik D. Photolysis of polycyclic aromatic hydrocarbons in water. Water Res 2001;35:233–43.
Nikolaou K, Masclet P, Mouvier G. Sources and chemical reactivity of polynuclear aromatic hydrocarbons in the atmosphere. Sci Total Environ 1984;32:103–32.
Niu J, Sun P, Schramm KW. Photolysis of polycyclic aromatic hydrocarbons associated with fly ash particles under simulated sunlight irradiation. J Photochem Photobiol A Chem 2007;186:93–8.
Pennise DM, Kamens RM. Atmospheric behavior of polychlorinated dibenzo-*p*-dioxins and dibenzofurans and the effect of combustion temperature. Environ Sci Technol 1996;30:2832–42.
Ram K, Anastasio C. Photochemistry of phenanthrene, pyrene, and fluoranthene in ice and snow. Atmos Environ 2009;43:2252–9.
Readman JW, Mantoura RF, Rhead MM. The physico-chemical speciation of polycyclic aromatic hydrocarbons (PAH) in aquatic systems. Fresenius' Z Anal Chem 1984;319:126–31.

Rockne KJ, Taghon GL, Kosson DS. Pore structure of soot deposits from several combustion sources. Chemosphere 2000;41:1125–35.
Sabaté J, Bayona JM, Solanas AM. Photolysis of PAHs in aqueous phase by UV irradiation. Chemosphere 2001;44:119–24.
Schmidt MW, Noack AG. Black carbon in soils and sediments: analysis, distribution, implications and current challenges. Global Biogeochem Cycles 2000;14:777–93.
Tham YWF, Sakukawa H. Preliminary study of the photolysis of fluorene in rainwater. Bull Environ Contam Toxicol 2007;79:670–3.
Wang D, Chen J, Xu Z, Qiao X, Huang L. Disappearance of polycyclic aromatic hydrocarbons sorbed on surfaces of pine [*Pinua thunbergii*] needles under irradiation of sunlight: volatilization and photolysis. Atmos Environ 2005;39:4583–91.